Surface-Initiated Atom Transfer Radical Polymerization from $Mg(OH)_2$ Nanoparticles to Prepare the Well-Defined Polymer-$Mg(OH)_2$ Nanocomposites

Ming-Jen Chang,[1] Jen-Yun Tsai,[1] Chia-Wei Chang,[1] Hwai-Ming Chang,[1] George J. Jiang[2]

[1]*Department of Chemistry and Center of Nano-Technology, Chung Yuan Christian University, Chung Li, Taiwan 32023, Republic of China*
[2]*Department of Chemical and Material Engineering, National Ilan University, Ilan, Taiwan, Republic of China*

Received 20 March 2006; accepted 2 November 2006
DOI 10.1002/app.25742
Published online in Wiley InterScience (www.interscience.wiley.com).

ABSTRACT: Well-defined polymer-$Mg(OH)_2$ nanocomposites were prepared by atom transfer radical polymerization (ATRP). The ATRP initiators were covalently attached to the $Mg(OH)_2$ by esterification of 2-chloropropionyl chloride with hydroxyl group. The amount of polymer grafted from $Mg(OH)_2$ can be controlled using a different catalyst system and adding a small amount of polar solvent. The well-defined diblock copolymer, consisting of poly(styrene) (PS) and poly(methyl methacrylate) (PMMA) were synthesized. The products were characterized by nuclear magnetic resonance, Fourier transform infrared, differential scanning calorimetry, and thermal gravimetric analysis. The morphologies of PS/PMMA and PS/PMMA/$Mg(OH)_2$-*g*-PS-*b*-PMMA blends are compared by using a scanning electron microscope. © 2006 Wiley Periodicals, Inc. J Appl Polym Sci 103: 3680–3687, 2007

Key words: $Mg(OH)_2$; ATRP; polymer nanocomposite

INTRODUCTION

$Mg(OH)_2$ is extensively adopted as a flame-retardant additives in polymers because it has a high endothermic decomposition temperature and low cost.[1–3] $Mg(OH)_2$ is more environmental friendly than halogen-based flame-retardants and has excellent smoke suppressing properties. The use of $Mg(OH)_2$ as a flame-retardant has some shortcomings. Many investigations have established that $Mg(OH)_2$ loadings of more than 60% by weight are generally required to confer an adequate level of flame retardency in polymer. However, such high loadings significantly degrade the mechanical properties of the polymer, because the compatibility between the filler and the polymer substrate is poor. Modifying the surface and reducing the size of the $Mg(OH)_2$ specimen are the most important methods for improving compatibility and solving this problem.

Surface modification of inorganic nanoparticles by chemically bonded has attracted increasing attention in recent years.[4–8] This interest is partly driven by a fundamental study of interfacial phenomena and also by the prospect of improved surface wettability and lubricity, and dispersion of particulates. Known methods for grafting polymer chains to particle surfaces including chemisorption of reactive polymer end group to the surface, grafting a polymer chain through a monomer covalently linked to the surface, or grafting a polymer chain from a surface modified with polymerization initiators. In the grafting process, a ''controlled/living'' polymerization method would be optimal, because such methods afford control over the molecular weight, the molecular weight distribution, and the structure of resulting polymer. Atom transfer radical polymerization (ATRP) is one of the most successful ''controlled/living'' polymerization methods that have developed in recent years.[9–12] Several groups have demonstrated that ATRP is very versatile and is tolerant of a wide range of functional groups present in the monomer, solvent, or initiator. ATRP has been adopted to prepare a wide range of architectures, including those of block, star, gradient and statistical copolymers, as well as well-defined macromonomers.

Metal oxide, such as SiO_2 and Fe_2O_3, nanoparticles are most used for surface-initiated polymerization. In this field, there are few papers using $Mg(OH)_2$ nanoparticle as a core to synthesis polymer-$Mg(OH)_2$ nanocomposites.[13] This investigation reports structurally well-defined polymer-nanoparticle hybrid that were prepared by modifying the surface of $Mg(OH)_2$ with 2-chloropropionyl chloride as an initiator for ATRP reaction (Scheme 1). The effect of the solvent and ligand on the efficiency of the reaction is discussed in this study. The well-defined diblock copolymer shell, consisting of diblock copolymer of poly(styrene) (PS) and poly(methyl methacrylate) (PMMA) were synthesized to confirm the existence of ''living'' chain ends. Microscopic studies reveal the

Correspondence to: G. J. Jiang (george@niu.edu.tw).

Journal of Applied Polymer Science, Vol. 103, 3680–3687 (2007)

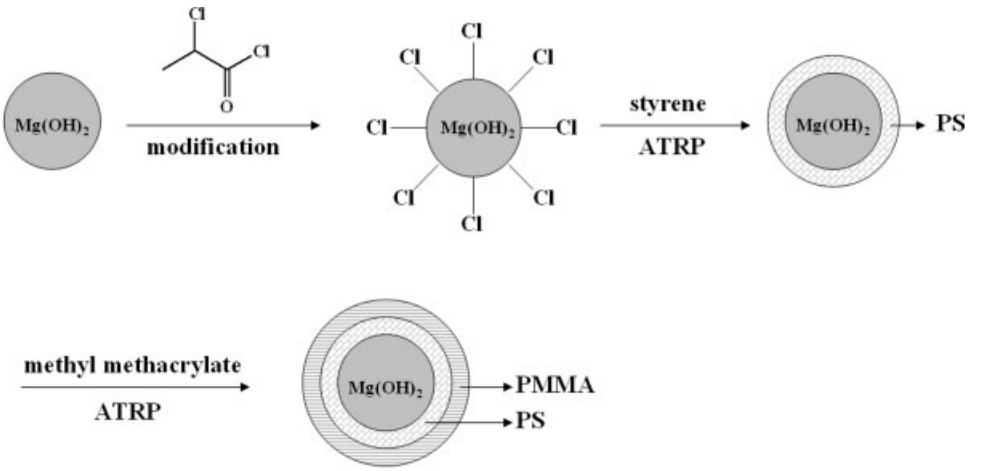

Scheme 1 The synthetic route of $Mg(OH)_2$-*g*-PS-*b*-PMMA nanocomposites.

effectiveness of adding $Mg(OH)_2$-*g*-PS-*b*-PMMA as a compatibilizer to the polymer blend PS/PMMA, which reduces the phase separation and promotes interfacial interaction between domains.

METHODS

CuCl (Merck, 99%), *N*,*N*,*N*′,*N*′,*N*″-pentamethyldiethylenetriamine (PMDETA) (Aldrich, 99%), and 2-chloropropionyl chloride (Fluka, 95%) were used without further purification. 2,2-Bipiridyl (Bpy) (Fluka, 98%) was purified by recrystallization from *n*-hexane. Styrene and methyl methacrylate were passed through a column that was filled with aluminum oxide to remove the inhibitor. $Mg(OH)_2$ nanoparticles (70 nm) were obtained from Desun Co.

Attachment of initiators to $Mg(OH)_2$

The functional initiator, 2-chloropropionyl chloride, was used as the modified reagent in the ATRP reaction on the $Mg(OH)_2$ surface. 0.5 g $Mg(OH)_2$ nanoparticles and 20 mL toluene were mixed and stirred vigorously about 10 min to ensure thorough dispersion. 2-chloropropionyl chloride was added to the reactor and all the modified reactions proceeded in a drying tube filled with $MgSO_4$. The polymerization reactions for different durations at various temperatures and various concentrations were observed. The thermal gravimetric analysis (TGA) results of the products were used to calculate the values of the modifying agent on the $Mg(OH)_2$ surface.

Synthesis of $Mg(OH)_2$-*g*-PS particle

About 0.5 g initiator-attached $Mg(OH)_2$ (4.25×10^{-4} mol Cl), 0.041 g CuCl (4.25×10^{-4} mol), 0.131 g 2,2-bipridyl (8.5×10^{-4} mol) or 0.147 g PMDETA (8.5×10^{-4} mol), and 13.278 g styrene (0.127 mol) were placed in three glass ampoules and degassed with three vacuum/nitrogen cycles. In some experiments, small amounts of solvent with different polarity index were added. All reactions were conducted under nitrogen at 80–110°C for 48–96 h. The reactions were terminated by adding the methanol and washing several times by water and methanol to remove remnant monomer and oligmer. The products of the $Mg(OH)_2$-*g*-PS particle were dried in a vacuum oven at 50°C.

Synthesis of $Mg(OH)_2$-*g*-PS-*b*-PMMA nanocomposite

Approximately 0.25 g $Mg(OH)_2$-*g*-PS macroinitiators (2.125×10^{-4} mol Cl), 0.041 g CuCl (4.25×10^{-4} mol), 0.147 g PMDETA (8.5×10^{-4} mol), 6.38 g MMA (0.064 mol), and 20 mL THF were placed in three glass ampoules and degassed during three vacuum/nitrogen cycles. All reactions were conducted under nitrogen at 60°C for 24–48 h. The reactions were

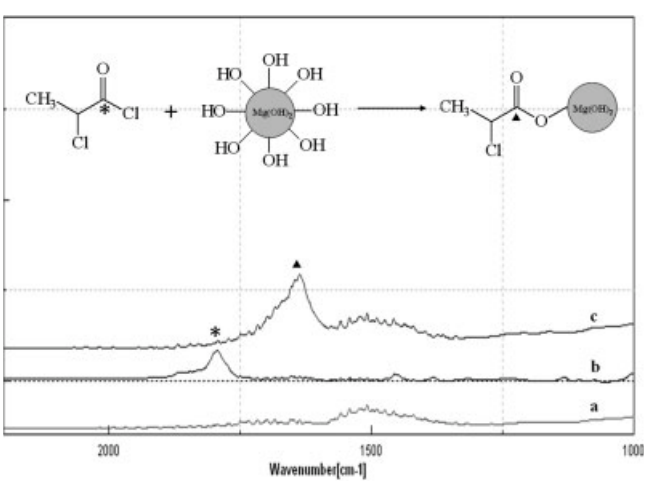

Figure 1 FTIR spectra of (a) pure $Mg(OH)_2$ nanoparticle, (b) 2-chloropropionyl chloride, and (c) initiator-attached $Mg(OH)_2$.

TABLE I
Reaction Parameters for Attachment of Initiators to $Mg(OH)_2$

No.	T (°C)	Time (h)	Molar ratio of I/M[a]	Residue (%) (500°C)[b]	Modified content (%)[c]
AC16	25	0.5	1	64.60	8.19
AC15	25	4	1	63.58	9.21
AC18	25	12	1	60.00	12.79
AC19	25	24	1	48.94	23.85
AC22	10	4	1	65.91	6.88
AC20	50	4	1	62.59	10.2
AC21	80	4	1	52.48	20.31
AC24	25	4	0.5	62.37	10.42
AC23	25	4	2	62.08	10.71

[a] I/M = 2-chloropropionyl chloride/$Mg(OH)_2$.
[b] The value of residue at 500°C were determined by TGA.
[c] Modified content = The residue at 500°C before modified (72.79%) − the residue at 500°C after modified.

terminated by methanol and washed three times by water and methanol. The products were dried in a vacuum oven at 50°C to yield the $Mg(OH)_2$-*g*-PS-*b*-PMMA nanocomposites. The diblock copolymer of PS and PMMA were characterized by nuclear magnetic resonance (NMR) to calculate the molar ratio of PS and PMMA. The TGA and differential scanning calorimetry (DSC) data specify the formation of diblock-copolymer shells.

Cleavage of PS from $Mg(OH)_2$

The $Mg(OH)_2$-*g*-PS hybrid particles were detached from the $Mg(OH)_2$ surface via transesterification. About 0.2 g $Mg(OH)_2$-*g*-PS hybrid particles were suspended in 10 mL THF, and 0.1g of Aliquot 336 was added as a phase transfer catalyst. A 10 mL of 40% aqueous HF was then added, and the mixture was stirred at ambient temperature overnight. PS was isolated by precipitation into methanol and dried in the vacuum. Molecular weights of PS were determined by using waters size exclusion chromatography (SEC) system with THF as eluent (1 mL/min) at 30°C with differential refractive index detection.

TABLE II
The Amount of PS Grafted from $Mg(OH)_2$ in the Different Reaction Condition of ATRP[a]

Run	T (°C)	Time (h)	Solvent[b]	Ligand	PS (%)[c]
AS1a8	80	72	–	Bpy	None
AS26	80	48	–	PMDETA	28.11
AS21	80	72	THF	Bpy	13.04
AS22	80	72	H_2O	Bpy	9.19
AS23	80	72	Toluene	Bpy	3.44
AS19	110	72	–	Bpy	26.00
AS20	110	96	–	Bpy	51.53
AS29	110	60	–	PMDETA	69.23
AS27	110	72	–	PMDETA	69.04

[a] All the ATRP reaction use AC15 (25°C, 4 h) as macroinitiator.
[b] Polarity index of THF = 4, H_2O = 9, toluene = 2.4, and the ratio of $Mg(OH)_2$/monomer/solvent = 0.5 g/13.278 g/0.1 mL.
[c] The amounts of grafted PS were calculated using TGA.

RESULTS AND DISCUSSION

Attachment of initiators to $Mg(OH)_2$

Esterification of $Mg(OH)_2$ with 2-chloropropionyl chloride yields a compound with reactive species to initiate the ATRP reaction for vinyl monomers. Figure 1 presents Fourier transform infrared (FTIR) spectra of $Mg(OH)_2$ nanoparticles, 2-chloropropionyl chloride, and initiator-attached $Mg(OH)_2$. The —C=O group of 2-chloropropionyl chloride appears at 1790 cm^{-1} [Fig. 1(b)] but shifts to 1630 cm^{-1} after esterification to form initiator-attached $Mg(OH)_2$ [Fig. 1(c)]. This result establishes that the bonding between 2-chloropropionyl chloride and $Mg(OH)_2$ nanoparticles is covalent bonds but not adsorption. Table I presents the degrees of modification with different reaction parameters. The results show that the modified content

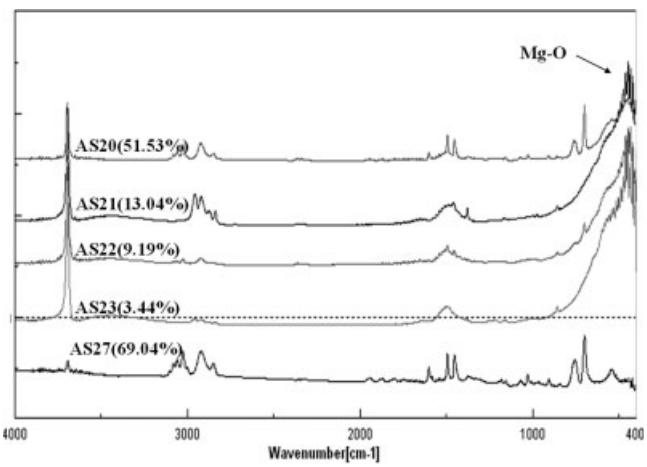

Figure 2 FTIR spectra of $Mg(OH)_2$-*g*-PS with different amount grafted PS.

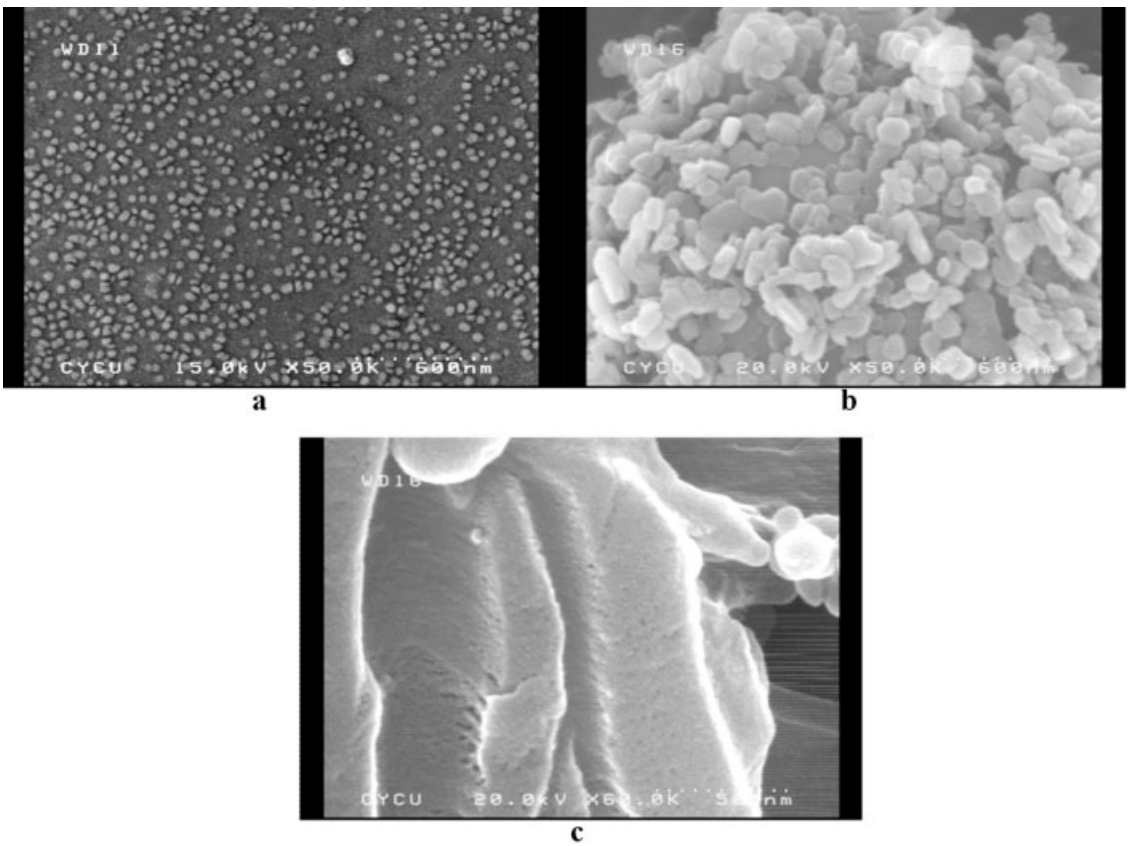

Figure 3 SEM pictures of (a) pure $Mg(OH)_2$ nanoparticle (70 nm), (b) 51.53% PS (AS20), and (c) 69.04% PS (AS27).

increases with the reaction time (run AC15, AC16, AC18, and AC19) and the temperature (run AC15, AC20, AC21, and AC22). However, changes in the concentrations of 2-chloropropionyl chloride do not markedly affect the modified content (run AC15, AC23, and AC24).

$Mg(OH)_2$-*g*-PS particles

The efficiency of the ATRP to synthesize the $Mg(OH)_2$-*g*-PS particles is the key procedure in the whole nanocomposite synthesis. The relative amount of grafted polymer compared with that of $Mg(OH)_2$ was determined by TGA. Table II presents the results including some important information. The ATRP reactions are undertaken using Bpy and PMDETA as a ligand. In the CuCl/Bpy system, the reaction of ATRP does not proceed at 80°C when using bulk polymerization. The initiator-attached $Mg(OH)_2$ cannot initiate the ATRP reaction since the reactions are heterogeneous. However, although the CuCl/PMDETA system still has an immiscible interface between organic and inorganic materials, the reaction rate can be increased above that of the CuCl/Bpy system. The activity of *N*-based ligands in ATRP increases with the number of the nitrogen atoms in the ligand and provide more coordinating sites to obtained better graft efficiency.[14] However, if small amounts of polar solvents, such as THF, H_2O, and toluene are added, then the ATRP reaction can be accelerated. The most likely explanation for the increased in the rate of ATRP in polar solvent is that the presence of more electrons rich environment leads to the formation of the more active Cu I catalyst, and increases the rate of active reaction.[15–17] At the higher temperature 110°C, the ATRP reaction proceeds successfully with Bpy or PMDETA as a ligand in bulk polymerization. FTIR and scanning electron microscope (SEM) can prove that the ''grafting from'' reaction proceed successfully. The

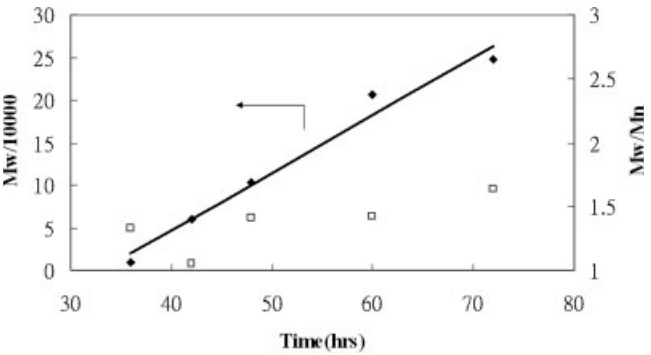

Figure 4 Dependence of M_w and M_w/M_n on reaction time for the ATRP of styrene from $Mg(OH)_2$ nanoparticles. Experimental conditions: [monomer] : [initiator] : [CuCl] : [PMDETA] = 300 : 1 : 1 : 2 in bulk polymerization at 110°C.

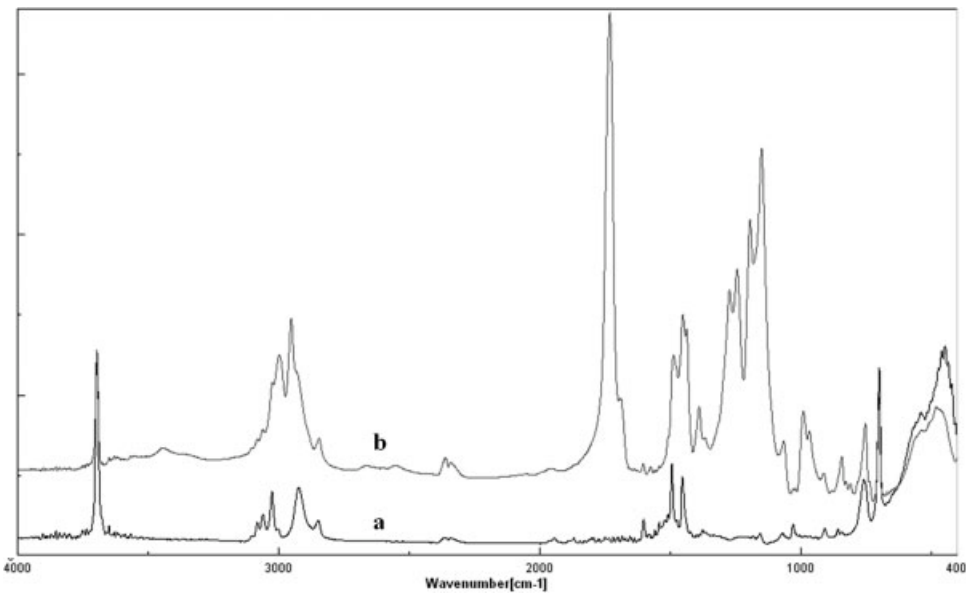

Figure 5 FTIR spectra of (a) $Mg(OH)_2$-*g*-PS and (b) $Mg(OH)_2$-*g*-PS-*b*-PMMA.

FTIR spectra (Fig. 2) indicate that the peak of Mg-O at 460 cm^{-1} disappears when a large amount of grafted polymer is obtained, because the thickness of the graft polymer exceeds the depth of penetration of IR source. The morphologies of pure $Mg(OH)_2$ nanoparticles and $Mg(OH)_2$-*g*-PS with different amounts of grafted polymer were investigated using SEM (Fig. 3). Figure 3(a) revealed that pure $Mg(OH)_2$ nanoparticles are spherical and having a uniform size about 70 nm. The modified $Mg(OH)_2$ nanoparticles were used as macroinitiators in the ATRP reaction. Therefore, much larger particles are obtained when the polymer chains grow from the $Mg(OH)_2$ surface. Figure 3(b) shows that the $Mg(OH)_2$-*g*-PS with lower conversion is still maintain spheroid. The results show that the polymer chains grafting from the $Mg(OH)_2$ surface. Figure 3(c) presents the more converted sample. The compacted and large amounts of polymer chains ''clothe'' the $Mg(OH)_2$ nanoparticles and become bulk materials. As expected, the bulk materials with

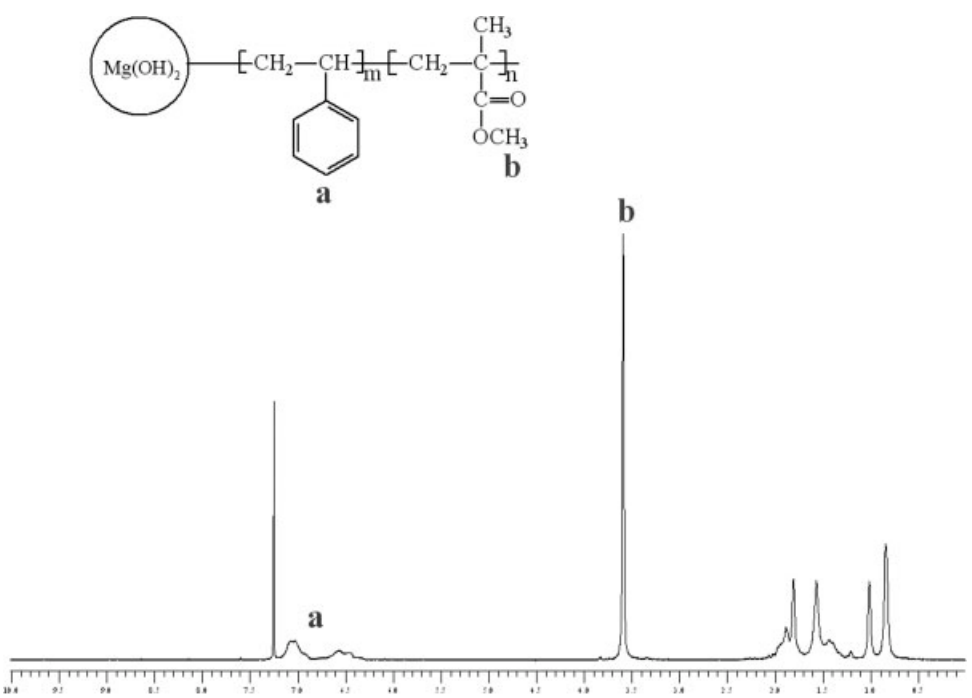

Figure 6 The ^{1}H-NMR spectrum of $Mg(OH)_2$-*g*-PS-*b*-PMMA.

TABLE III
Properties of $Mg(OH)_2$-*g*-PS-*b*-PMMA Nanocomposites[a]

No.	Macroinitiator	Time (h)	PS content[b]	PMMA content[b]	T_d (°C)	T_g (°C)
AS20	–	–	1	0	356.1	83.9
ASC20-36	AS20	36	1	3.14	338.5	127.2
ASC20-48	AS20	48	1	5.14	339.1	127.4
AS27	–	–	1	0	390.3	106.7
ASC27-24	AS27	24	1	0.39	376.4	109.1/131.6
ASC27-36	AS27	36	1	0.79	373.1	109.1/130.2
ASC27-48	AS27	48	1	10.46	340.4	129.3

[a] Experimental conditions: temperature 60°C, solvent THF 20 mL, [MMA] : [CuCl] : [PMDETA] = 150 : 1 : 2.
[b] The ratio of PS and PMMA were determined using ^{1}H-NMR.

chemically bonded between organic and inorganic has better properties than traditional composites.

Information about the molecular weights and molecular weight distributions of the grafted PS were gained by etching the $Mg(OH)_2$ core. In this section, the ATRP reactions are undertaken in CuCl/PMDETA system at 110°C for 36–72 h. The molecular weights measured by SEC increase linearly with reaction time, and the molecular weight distributions (M_w/M_n) are relatively low (< 1.6). The results revealed that the graft polymerization of styrene from $Mg(OH)_2$ surface via ATRP is a ''living''/controlled polymerization. Figure 4 shows the molecular weight and molecular weight distributions versus reaction time for ATRP of PS from $Mg(OH)_2$ nanoparticle.

$Mg(OH)_2$-*g*-PS-*b*-PMMA nanocomposite

The ''living'' chain ends of $Mg(OH)_2$-*g*-PS macroinitiator are served as surface-initiated of ATRP to synthesize the PS-*b*-PMMA diblock copolymer.[18–21] The composition of the $Mg(OH)_2$-*g*-PS-*b*-PMMA was characterized by FTIR and proton NMR spectroscopy. Figure 5 presents the FTIR analysis of the $Mg(OH)_2$-*g*-PS and $Mg(OH)_2$-*g*-PS-*b*-PMMA nanocomposites. The most interesting characteristic of the FTIR spectra of $Mg(OH)_2$-*g*-PS-*b*-PMMA is the appearance of adsorption peaks at 1710 cm^{-1} and 1100–1400 cm^{-1}, which are characteristic peaks of PMMA. The molar ratio of PS and PMMA in the $Mg(OH)_2$-*g*-PS-*b*-PMMA nanocomposites can be calculated from NMR spectra (Fig. 6). The aromatic units from the PS block can be assigned to the peak of 6.3–7.2 ppm, and the —OCH_3 units from the PMMA block can be assigned to the peak of 3.6 ppm. Table III shows the diblock copolymer can be synthesized successfully in two different macroinitiators, AS20, which contains 48.47% of $Mg(OH)_2$, and AS27, which contains 30.96% of $Mg(OH)_2$. In the AS20 macroinitiator, the PMMA block content increases with the polymerization time. The thermal properties, including T_d and T_g, establish the formation of the diblock copolymer.[18–21] The T_d shifts downward and the T_g shifts upward as anticipated for the PMMA block. Only one T_g is observed and explained below (Fig. 7). Comparing the normal diblock copolymer, the polymer chain of PS in the $Mg(OH)_2$-*g*-PS-*b*-PMMA was fixed between $Mg(OH)_2$ and the PMMA block. This result confines the flexure of PS block and leads to the unapparent T_g when the large amount of PMMA block was grafted. All of the thermal properties of the PS block weakly affect the

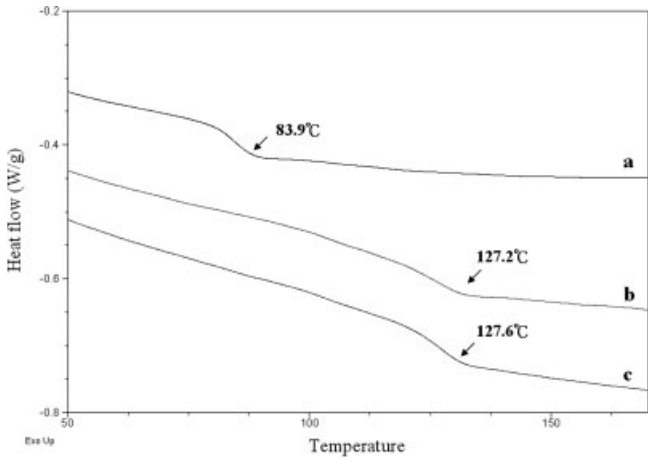

Figure 7 The DSC curves of (a) AS20, (b) ASC20-36, and (c) ASC20-48.

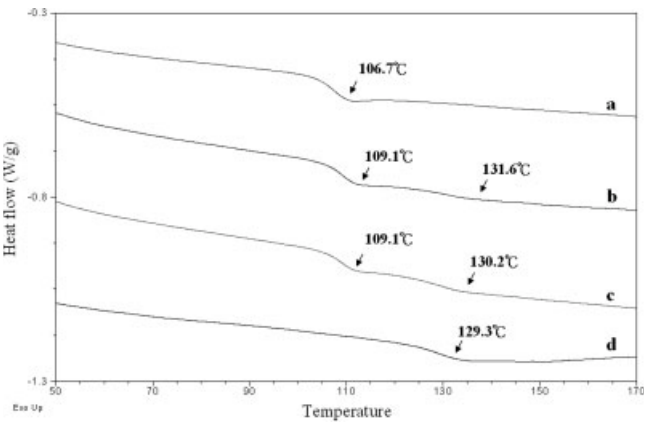

Figure 8 The DSC curves of (a) AS27, (b) ASC27-24, (c) ASC27-36, and (d) ASC27-48.

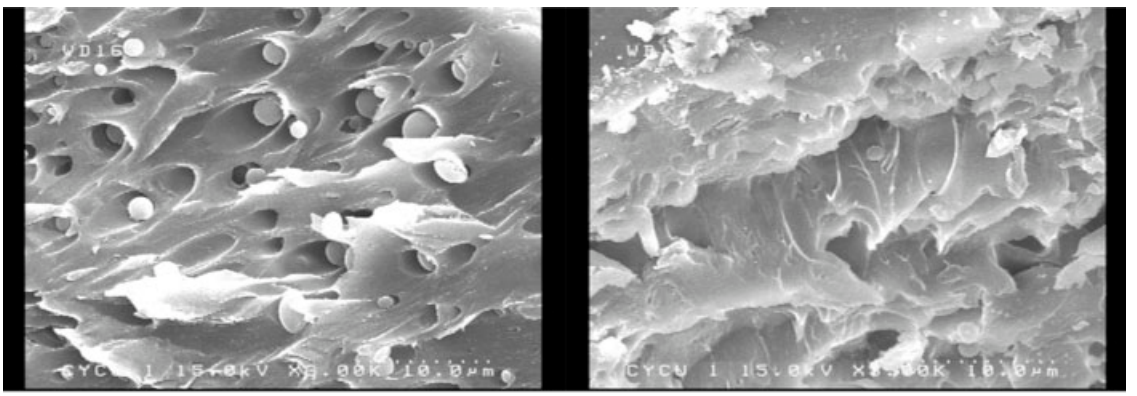

a b

Figure 9 The SEM micrographs of (a) PS/PMMA blend [50/50 wt %] and (b) PS/PMMA/$Mg(OH)_2$-*g*-PS-*b*-PMMA blend [50/50/20 wt %].

$Mg(OH)_2$-*g*-PS-*b*-PMMA because the amount of PS is small.

In the AS27 macroinitiator, the contents of the PMMA block increases with the reaction time but exceed the linearly living polymerization character in the ASC27-48. It is probably due to the autoacceleration caused by the sudden elevation of viscosity, and leads to a rapidly increasing rate of polymerization. T_d in the ASC27 series exhibits the same change, declining by 17°C for ASC27-36 and even 50°C for ASC27-48, because the PMMA block content is high. ASC27-24 and ASC27-36 exhibit two glass transition regions, $T_{g,PS} = 109$°C, associated with the PS block, and $T_{g,PMMA} = 130$°C, associated with the PMMA block (Fig. 8). A small amount of PMMA block reduces the ''confinement effect'' and two T_g values can be observed apparently. All of the thermal properties demonstrate that the well-defined $Mg(OH)_2$-*g*-PS-*b*-PMMA nanocomposites can be synthesized successfully using ATRP technology.

PS/PMMA and PS/PMMA/$Mg(OH)_2$-*g*-PS-*b*-PMMA blends

The morphology of PS/PMMA and PS/PMMA/$Mg(OH)_2$-*g*-PS-*b*-PMMA blends formed by solution blending was studied, using scanning electron microscopy. Figure 9(a) shows SEM micrographs of the fractured cross section surface of PS/PMMA with a 50/50 weight ratio. Figure 9(b) shows that 20 wt % of $Mg(OH)_2$-*g*-PS-*b*-PMMA was added as a compatibilizer in the PS/PMMA blend. In the homopolymer blend, the polymers are grossly phase-separated and poorly dispersed domains at the fracture surface, as shown in Figure 9(a). The lack of adhesion between PS and PMMA is evident, wherein dispersed particles do not adhere to the PS and leave cavities with a smooth surface. The similar blend that contains $Mg(OH)_2$-*g*-PS-*b*-PMMA has a totally different morphology, as shown in Figure 9(b). The presence of $Mg(OH)_2$-*g*-PS-*b*-PMMA is associated with in a more homogeneous morphology. The use of the coreactive diblock copolymers imparted significant changes on the phase morphology, with a substantial decrease in phase size. $Mg(OH)_2$-*g*-PS-*b*-PMMA is clearly an effective compatibilizer in the PS/PMMA blends.

CONCLUSIONS

Structurally well-defined polymer-nanoparticle hybrids were prepared by ATRP through modifying the surface of $Mg(OH)_2$ nanoparticles as an initiators. The polymerization of styrene displayed the amount of PS grafted from the $Mg(OH)_2$ surface can be increased by using the CuCl/PMDETA system and adding a small amount of polar solvent. FTIR spectra and SEM images presents the successful proceeding of the ''graft from'' reaction. In the meanwhile, polymerizations of styrene using the nanoparticle initiators showed the diagnostic criteria for a ''living''/controlled radical polymerization in CuCl/PMDETA system. Additionally, the synthesis of a diblock copolymer shell using an $Mg(OH)_2$-*g*-PS as macroinitiator demonstrates the existence of ''living'' chain ends. The morphology of polymer blends establishes the effectiveness of $Mg(OH)_2$-*g*-PS-*b*-PMMA in the PS/PMMA blends by improving dispersion and increasing interfacial interaction between domains. Significantly, this procedure can be extendable to any polymer that can be grafted from an initiator bound to inorganic materials.

References

1. Wang, Z.; Qu, B.; Huang, P. J Appl Polym Sci 2001, 81, 206.
2. Wang, Z.; Shen, X.; Fan, W. Polym Int 2002, 51, 653.
3. Tai, C. M.; Li, R. K. Y. J Appl Polym Sci 2001, 80, 2718.

4. Gu, B.; Sen, A. Macromolecules 2002, 35, 8913.
5. Chen, X. Y.; Armes, S. P.; Greaves, S. J. Langmuir 2004, 20, 587.
6. Vestal, C. R.; Zhang, Z. J. J Am Chem Soc 2002, 124, 14312.
7. Werne, T. V.; Patten, T. E. Langmuir 2001, 17, 4479.
8. Liu, T.; Jia, S.; Kowalewski, T.; Matyjaszewski, K. Langmuir 2003, 19, 6342.
9. Matyjaszewski, K.; Patten, T. E.; Xia, J. J Am Chem Soc 1997, 119, 674.
10. Schon, F.; Hartenstein, M.; Muller, A. H. E. Macromolecules 2001, 34, 5394.
11. Matyjaszewski, K.; Paik, H. J.; Zhou, P.; Diamanti, S. J. Macromolecules 2001, 34, 5125.
12. Matyjaszewski, K.; Nanda, A. K. Macromolecules 2003, 36, 599.
13. Ok, J.; Matyjaszewski, K. J Inorg Organomet Polym Mater 2006, 16, 129.
14. Matyjaszewski, K.; Xia, J. Chem Rev 2001, 101, 2921.
15. Wang, X. S.; Armes, S. P. Macromolecules 2000, 33, 6640.
16. Matyjaszewski, K.; Nakagawa, Y.; Jasieczek, C. B. Macromolecules 1998, 31, 1535.
17. Haddleton, D. M.; Heming, A. M.; Kukulj, D. Macromolecules 1998, 31, 2016.
18. Xu, F. J.; Cai, Q. J.; Kang, E. T. Langmuir 2005, 21, 3221.
19. Cui, T.; Zhang, J.; Wang, J.; Cui, F.; Yang, B. Adv Funct Mater 2005, 15, 481.
20. Krishnan, R.; Srinivasan, K. S. V. J Appl Polym Sci 2005, 97, 989.
21. Wang, Y. P.; Pei, X. W.; He, X. Y. Eur Polym J 2005, 41, 1326.